43rd AIAA Aerospace Sciences Meeting and Exhibit
10-13 January 2005, Reno, Nevada

AIAA 2005-950

Inductively Coupled Plasmas Supported by Laser Plasmas for High Enthalpy Flow

Takayoshi Inoue [*],Susumu Uehara.[†], Kimiya Komurasaki [‡] and Yoshihiro Arakawa [§]

University of Tokyo, Bunkyo-ku, Tokyo, 113-8656, JAPAN

In this study a fundamental study on stability of an atmospheric inductively coupled plasma generator (ICPG) for high-enthalpy and high-stagnation pressure flow were conducted. Whereas ICPG is expected to be used as a simulator of the planetary entry flowfield, the existing ICPGs have been operated with the pressure of less than 1 atm. We demonstrated the generation of ICPs with the pressure of more than 1 atm and it was found that the operational conditions strongly depend on the design of the tangential flow injection ring and the pressure. It was also successfully demonstrated that Laser Sustained Plasma (LSP) could be applied to the ICP stabilization. Especially a double tube configuration will provide a wide range of the capability to stabilize the ICPs.

Nomenclature

A_t	=	the cross section of the orifice
C_p	=	capacitance of the capacitor connected in parallel to the load coil
H_∞	=	specific enthalpy of the flow
h_w	=	specific enthalpy of the flow at the TPS surface
K	=	proportional constant of the recession rate of the TPS materials
M	=	mutual indactance
$\dot{m}$	=	recession rate of the ablative TPS material
$\dot{m}_{A,B,C}$	=	mass flow rate supplied from the inlet A, B, C respectively
L_p	=	equivalent inductance of the inductively couple plasma
p_s	=	stagnation pressure of the flow
R	=	resistance of the impedance matching network
R_{Ar}	=	the gas constant of Argon
R_N	=	curvature radius of the TPS surface
R_p	=	equivalent resistance of the inductively coupled plasma
R'	=	resistance including that derived from the coupling with the inductively coupled plasma
σ	=	the critical flow coefficient(=0.726)
T_m	=	temperature of the gas going through the orifice
ω	=	RF angular frequency

I. Introduction

THIS work describes a fundamental study on an atmospheric inductively-coupled plasma generator for high-enthalpy and high-stagnation pressure flow, which is expected to play important role in thermal protection

[*] Graduate student, JSPS Research Fellow, Department of Aeronautics and Astronautics, University of Tokyo, 7-3-1 Hongo, Bunkyo-ku, Tokyo, 113-8656, JAPAN, Student Member AIAA.
[†] Graduate student, Department of Aeronautics and Astronautics, University of Tokyo, 7-3-1 Hongo, Bunkyo-ku, Tokyo, 113-8656, JAPAN, Student Member AIAA.
[‡] Associate Professor, Department of Advanced Energy, University of Tokyo, 7-3-1 Hongo, Bunkyo-ku, Tokyo, 113-8656, JAPAN, Member AIAA.
[§] Professor, Department of Aeronautics and Astronautics, University of Tokyo, 7-3-1 Hongo, Bunkyo-ku, Tokyo, 113-8656, JAPAN, Member AIAA.

Copyright © 2005 by the American Institute of Aeronautics and Astronautics, Inc. All rights reserved.

system development for re-entry capsules and planetary missions.

In 2002 the Solar System Exploration Decadal Survey (SSEDS) produced "New Frontiers in the Solar System: An Integrated Exploration Strategy", where they identified a broad range of science objectives and future missions for the next decade.[1] Some of the strategies of high priority are related with the compositional measurement of the surface and atmosphere of planets such as Mercury, Venus and so on. The most straightforward and reliable method should be in-situ probes and sample analysis by landers.

A body of probe vehicle in a very high enthalpy atmospheric flow is protected by the Thermal Protection System (TPS). Any trouble of the TPS can lead to a fatal mission failure since the TPS is a single point-of failure sub system. The predicted entry heating environments for probes to Jupiter, Venus and Neptune are very severe with peak heat flux of several dozen kW/cm^2 and with stagnation pressure of few atm. For these probes, the ablative TPS should be used, which amounted to 10 – 50 % of the probes in weight as was demonstrated in Galileo probe in 1995 and Pioneer probes in 1978.[2] Hence optimization of the TPS materials, its thickness and design will extend mission capability. Unfortunately it was pointed out that the TPS materials mounted in these missions should be re-qualified or may be unavailable.[3] Thereafter the development and sophisticated modeling of the TPS are significant issues and adequate ground test facilities have been needed.

The recession rate $\dot{m}$ of the ablation TPS can be expressed as follow;[4]

$$\dot{m} = K\sqrt{\frac{p_s}{R_N}}\left(H_\infty - h_w\right) \tag{1}$$

Here K is a proportional constant depending on the TPS materials, p_s is the stagnation pressure, H_∞ is the specific enthalpy of the flow. Equation (1) shows that the flow environments to evaluate the ablative TPS materials are characterized by two important parameters; stagnation pressure and specific enthalpy.

Arc heaters are the most popular devices, in which the pressure and the specific enthalpy are moderately high. On the other hand, erosion of electrodes contaminates the flow that prevents one from accurate investigation of the catalytic behavior and chemical reactions behind the shock wave.[5] Additionally it has disadvantages in dealing with carbon-compound gases), where the carbon is deposited on the insulator between the electrodes and cause short-circuiting.[6] The dominant component of the atmosphere of the Venus and the Mars is carbon dioxide. Hence the arc heaters involve difficulties to be operated as the aerothermal studies and flight enviroment simulations for the Venus and the Mars entry probes. Laub et.al. pointed out that the performance of high-density carbonaceous TPS materials and analytical scaling of their performance in air to the Venus atmosphere is straight forward since no existing arc jet facilities operate on CO_2.[3] From this view point, there need to be accumulation of the experimental data on the CO_2 high-enthalpy flow with high stagnation pressure.

In order to overcome the disadvantages of the arc heaters, a discharge with no electrode, especially Inductively Coupled Plasma Generator (ICPG), is supposed to be an alternative for the high enthalpy flow simulator.[7] Although ICPs has superior characteristics in the point of the contamination and capability to deal with active gases and the carbon-compound gases, the stagnation pressure is limited at low pressure while the expected stagnation pressure for the Venus probes is more than 1 atm.

An atmospheric ICPs have been enthusiastically investigated in various research fields like atomic emission spectrometry, mass spectrometry, plasma processing, and destruction of waste. It is responsible for such attentions that an uniform high enthalpy field is obtained over large volume without contamination of the flow. In the field of the astronautics the first research on ICP had conducted to simulate the heat transfer and flow characteristics of a Gas Core Nuclear Rocket with inductively coupled plasmas at NASA.[8-10] However, the operational characteristics of the ICPs with the pressure of more than 1atm have not been examined enough.

The prime objective of this study is to clarify the operational characreristics of the ICPG with the pressure of more than 1 atm. Second, since there was operational limitation related to the stabilization based on the tangential flow injection, a method by using a laser plasma was tested to stabilize the ICP.

II. Experimental Setup

A. ICP torch and impedance matching network

Figure 1 shows a schematic diagram of the experimental setup. A quartz glass tube of 22 mm in the inner tube diameter as the plasma-sustaining channel was supported by a set of holders made of stainless steel, enabling generation of the ICP and observation of the plasma. A water-cooled load coil, fabricated from 3 mm copper tubing,

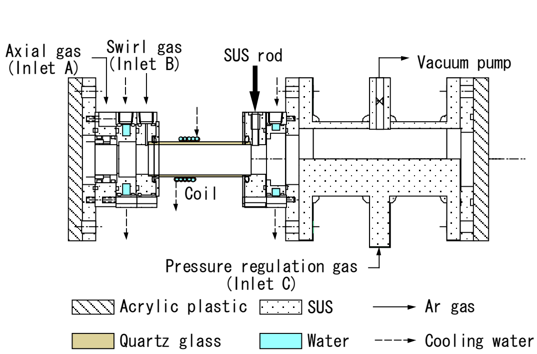

Figure 1. Schematic of the discharge tube.

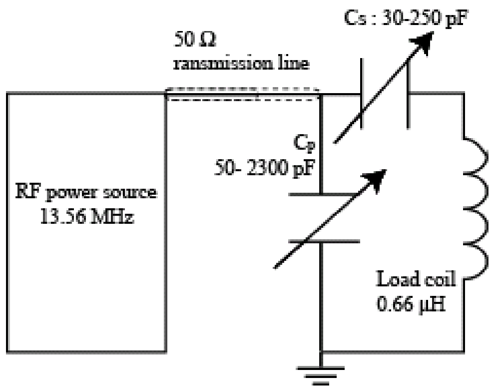

Figure 2. Impedance matching network.

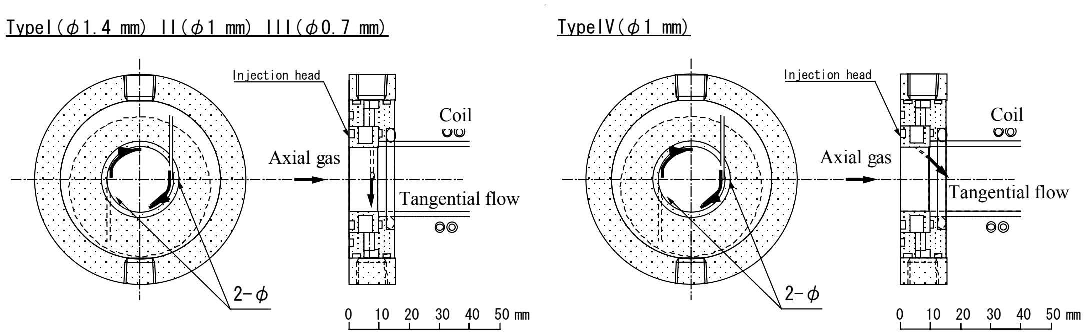

Figure 3. Design of the tangential flow injection rings

has an inside diameter of 30 mm and consists of 5 turns. The coating of the copper tubing with a thermal shrinkage tube eliminated the problem of the short-circuiting between respective turns. The work gas was pumped out through an orifice by an oil-sealed rotary vacuum pump in order to regulate the pressure in a wide rage, although most of the atmospheric ICP torches have been generated in an open tube.

The circuit diagram of an impedance matching network is shown in fig. 2. The matching circuit is composed of the load coil and two variable capacitors, which were adjusted manually. RF power generator with oscillation frequency of 13.56 MHz and maximum output power of 1.25 kW was utilized and connected to the network through 50 Ω co-axial transmission line. The forward power and the reflected power were read out from the RF power supply.

B. Swirl gas injection rings

As has been often seen in various researches, tangential flow injection has importance for the ICP generation. Herdrich et.al. studied the effects on the flow enthalpy and tube heat loads under low pressure of about several torr.[11] They measured the flow enthalpy and tube cooling power with changing the fraction of the tangential and the axial mass flow rate and resulted that the tangential flow played an essential role in the term of the efficiency. On the other hand some papers reported that there were certain operational instabilities or operational limits, thereafter the tangential gas injection is thought to have a decisive significance for ICP generation, especially for higher pressure.[6,11,12] Yabuta et.al. evaluated the inlet design of an ICP torch with the static pressure of 1 atm.[13] Although, in their investigation, the ICP stability was characterized by the diameter of the inlet, their interests was directed to atomic emission spectrometry and how to reduce mass consumption of work gas, so effect of the pressure on the stability was not studied.

In this study several injection rings, which have different inlet diameters and tangential angles, were tested. Figure 3 shows schematic of the rings used in this study. Type I-III have same tangential angle of $\pi/2$ to the axial direction with different inlet diameters; 1.4 mm, 1 mm, 0.7 mm respectively. Type IV has the tangential angle of $\pi/4$ and inlet diameter of 1mm.

C. CW CO_2 Laser device

In this study a fundamental study on the stabilization by laser plasmas was conducted by using a 2kW CW-CO2 laser (Panasonic YB-L200B7T4). The transverse mode of the laser beam is almost TEM_{00} but have an annular shape in its intensity distribution (Fig. 4). The beam divergence is less than 2 mrad at the laser exit. The beam diameter was magnified by factor of 2.2 using a ZnSe beam expander, and the expanded beam was condensed into the discharge tube through a ZnSe plano-convex lens. The focal length of the lens was 210 mm, corresponding to 6.3 in F-number (which was defined as focal length normalized by beam diameter).

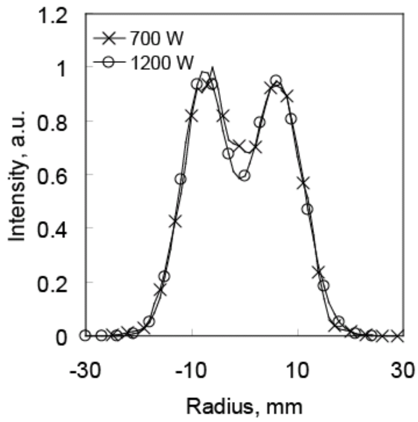

Figure 4. Transverse intensity distribution of the TEM_{00} CO2 laser.

D. Pressure regulation

In order to investigate the pressure effects on the ICP stability, it is effective to regulate the pressure without changing the tangential mass flow rate. Figure 1 also shows the conceptual diagram of gas flow for explaining the way to adjust experimental parameters. The gas flow supplied form inlet A and B goes through the discharge tube and that from inlet C does not. Assuming that the all of the gas are mixed completely and have a temperature T_m and the difference between stagnation pressure and static pressure can be negligible, the static pressure in the tube can be expressed as follows;

$$p_s = \frac{\sqrt{R_{Ar}T_m}}{A_t \sigma}\left(\dot{m}_A + \dot{m}_B + \dot{m}_C\right) \tag{2}$$

where σ is the critical flow coefficient (=0.726), R_{Ar} is the gas constant of Argon and A_t is the throat cross section of the choking orifice. Then equation (1) can be written as

$$p_s = \frac{\sqrt{R_{Ar}T_m}}{\left(A_t \Big/ \left(1 + \dfrac{\dot{m}_C}{\dot{m}_{A+B}}\right)\right)\sigma}\dot{m}_{A+B} \tag{3}$$

This equation represents that the effective throat cross section can be changed by the influx of the $\dot{m}_C$ so that the pressure regulation become enable without adjusting the tangential and axial gases $\dot{m}_{A+B}$. The static pressure in the chamber was measured with a semiconductor pressure transducer (Philips Sensor Technology Corp.: JS-24SHD-10).

III. Atmospheric ICP generation

A. Experimental procedure

Since the RF power was not enough to initiate atmospheric ICPs without ignitors, following procedures were taken;

a) Set the mass flow rate to 0 slm to decrease the pressure in the discharge tube.
b) Set the RF power output to 500 W resulting capacitively coupled plasma generation. [I]
c) Gradually increased the mass flow rate and pressure coming to about 1 atm the mode transition occurred and thermal plasma (ICP) was generated. [II]
d) Once the ICP were produced, the flow rate, the pressure and RF power could be adjusted without inductive-capacitive mode transition. [III]

Here the corresponding images of the plasmas are shown in fig. 5. In this study the power level of the devices is not so large so that that the work was Argon in spite of CO_2.

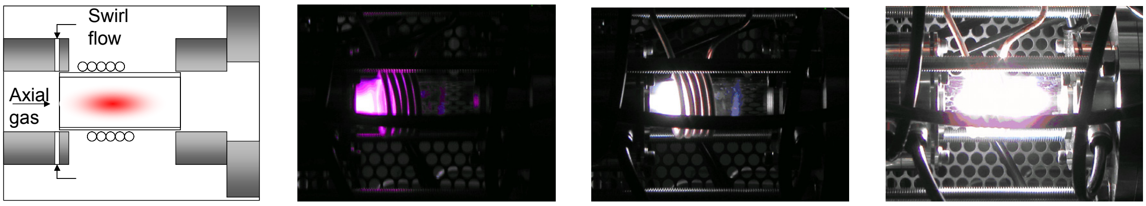

[Outline of the tube] [I] [II] [III]

Figure 5. Images of the generation of an ICP: [I] low-pressure capacitively coupled plasma, [II] inductively coupled plasma (<1atm), [III] inductively coupled plasma (>1 atm).

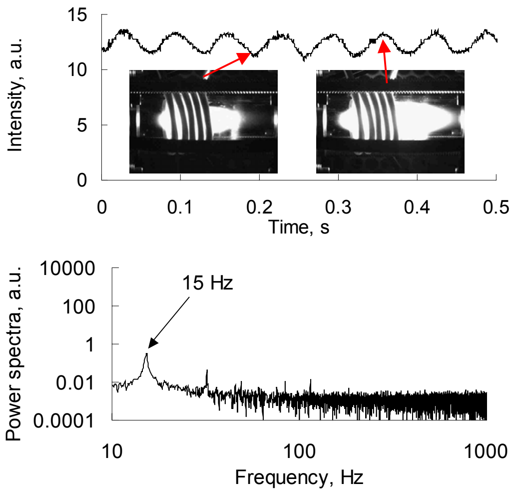

Figure 6. CCD images of the oscillating ICP and the time history of its luminescence (upper), and the power spectra of the oscillating luminescence(lower).

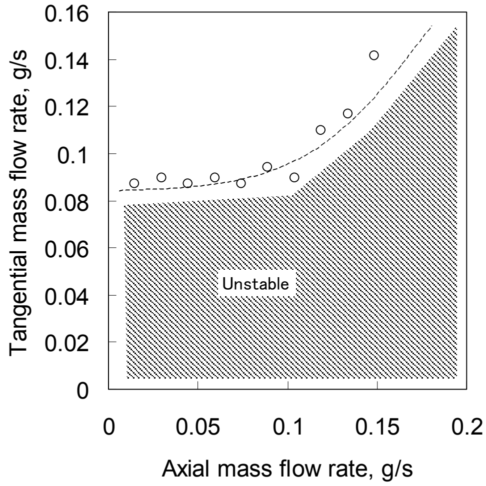

Figure 7. The minimum tangential mass flow rate as a function of the axial gas injection.

B. ICP instability

Experimental confirmed that the once generated thermal ICP was relatively stable so that there were hysteretic phenomena. However there existed operational limitation in the mass flow rate and RF power. When the condition was adjusted toward the operational limit, the ICP started to oscillate unstably and disappeared at the end. A CCD camera images, time history of the plasma luminance obtained by a photo-detector and its power spectra are shown in fig. 6.

Such instabilities were observed when the mass flow rate of the tangential flow was changed. Figure shows the minimum mass flow rate of the tangential flow for the stable generation of the ICPs as a function of the axial gas mass flow rate. In this case the pressure regulation was not conducted so that the pressure depended on the net mass flow rate of the tangential and axial flow. The result observed that the axial flow did not have any significant effect on the ICP stabilization. In the following experimental, the axial mass flow rate was set to 0 slm and *the mass flow rate* represents that of the tangential flow except as otherwise noted.

C. Stable conditions

Figure 8 shows the maximum and minimum mass flow rate with various static pressures. In this figure, the black dots and the open dots represent the maximum mass flow rate and the minimum mass flow rate to stably sustain the ICP. The ranges of the mass flow rate became narrower as the pressure increased. It was also found that, even if the RF power was increased, the minimum mass flow rate did not decrease while increase in RF power relaxed limit on the maximum mass flow rate considerably. Considering this tendency, the maximum and minimum limitations in the mass flow rate would be characterized by different physical mechanisms: the maximum one would arise from the lack in the power so that the work gas would not be ionized enough to absorb the RF power. On the contrary, insufficient swirl intensity would be responsible for the instability at lower mass flow rate.

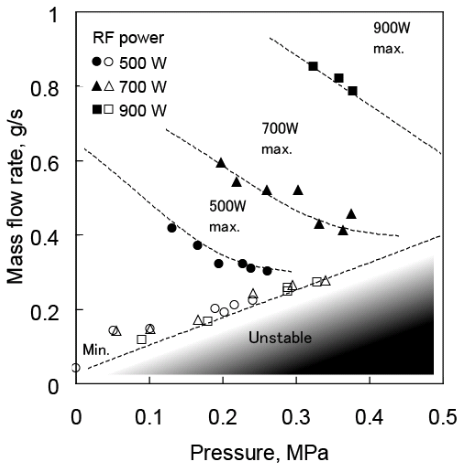

Figure 8. The operational range of mass flow rate for the stable ICPs generation. The black and open dots represent the maximum and the minimum mass flow rate of the tangential flow respectively.

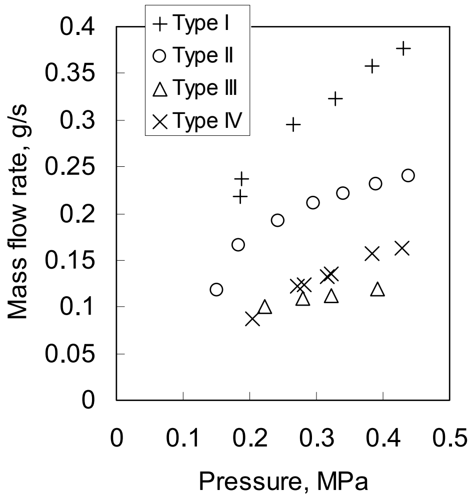

Figure 9. Minimum mass flow rate with various injection rings.

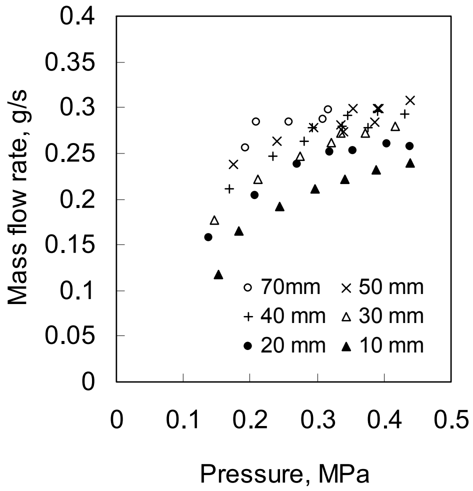

Figure 10. Minimum mass flow rate for various coil locations with the injection ring "Type II".

Herdrich et.al. described that there were some kind of instabilities in their experiments when the input power was increased resulting in the rise in the pressure.[11] Similar result was reported in other paper.[6] Based on the preceding consideration, the instabilities observed in their experiments would be the minimum in the mass flow rate to a certain pressure.

D. Effects of the design of the injection rings and the coil location

A common limitation of ICPGs operation has been often seen when one had tried to increase the RF power or to decrease the mass flow rate for higher enthalpy. Thereafter the instability for the lower mass flow rate would have much importance to clarify the operational characteristics. Figure 9 shows the minimum mass flow rate with several types of the injection ring geometries. The results present that the smaller diameter of the injection hole, the less the minimum mass flow rate, as expected. Using the injection ring that has smaller diameter of 0.5 mm, there was less instable behavior and no termination. However the ICP had gradually changed its shape with decreasing mass flow rate and had been off-axis configuration, leading to the over-heat load to the discharge tube. As to the effect of the angle of the injection port, there seems to be an optimum angel to obtain the tangential flow effects efficiently. In this study, though the several injection rings with different injection angles have prepared, it was difficult to test the injection rings due to the damage onto the discharge tube.

It can be easily expected that the tangential flow would decay along the discharge tube. So far the discharge coil being placed closed to the injection bores as possible and the distance between the injection ring and the first turn of the coil was about 10 mm. The influences of the decay on the ICP instability would provide useful information to discuss the physical background of it. Figure 10 shows that the minimum mass flow rate for various coil locations. The difference between the cases of 10 mm and 20 mm was significantly large and, as a whole, the minimum mass flow rate increase with the distance.

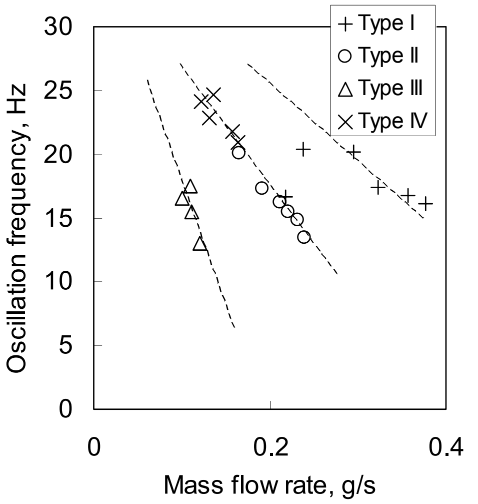

Figure 11. Oscillation frequency with various injection rings.

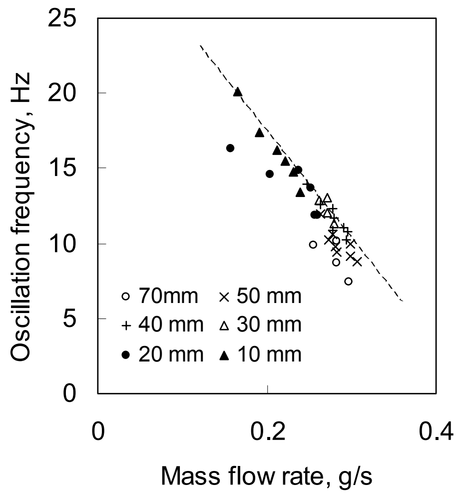

Figure 12. Oscillation frequency for various coil locations with the injection ring "Type II".

E. Oscillation frequency

As to the effects of the tangential flow on the ICP stability, there seems to be two different aspects; one is that the tangential flow produces lower pressure in the tube center,[11] the other is that the tangential flow makes the high temperature plasma region *float to the axis* because of the buoyancy force in the centrifugal field.[14] Figures 11 and 12 show the oscillation frequency of the RF reflected power during unstable ICP generation. Noteworthy is that the oscillation frequency was strongly related to the mass flow rate in spite of the plots being taken under various pressures (Fig. 12). Similar tendency can be seen in fig. 11, i.e. "Type II" and "Type IV" although the designs are different. On the other hand, the difference in the diameter of the injection bores caused evident change in the relation between the oscillation frequency and the mass flow rate. These results would provide an insight to understand the physical aspect of the instability.

IV. Stabilization by using Laser Plasmas

A. Principle of the stabilization

It was found that, as the pressure increased, the operational condition became limited in a certain range of the mass flow rate. Whereas the heat flux and the stagnation pressure should be measured, the limitation will cause performance limitations as the high enthalpy flow generator. In this study efforts were focused on the ICP stabilization and it was probed that the tangential flows govern the ICP stability.

In this section, attempts of the ICP generation without the tangential flow will be described. In order to produce the ICP stably, it is necessary that there exist a certain mechanism that makes ICP geometry axial symmetry and holds it on the axis. Laser-Sustained Plasmas (LSPs) can be one of the candidates due to LSP being easily generated in a higher pressure, and being compatible with the characteristic of electrodeless discharge of ICPs.

LSPs are generated by absorbing intense laser irradiation via inverse bremsstrahlung process. Figure 13 shows the absorption coefficient being strongly dependent on the pressure and being larger with the higher pressure.[15] Hence the threshold intensity to sustain LSPs decreases

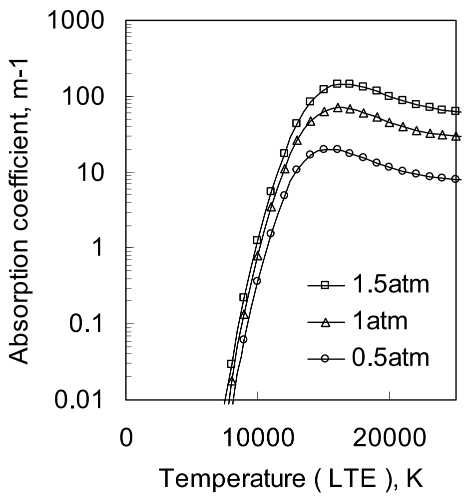

Figure 13. Absorption coefficient of Ar plasma to the 10.6 μm laser irradiation.

with the increase in the pressure around atmospheric pressure. However laser discharge seems not to be useful to produce high enthalpy flow directly since the energy conversion efficiency of the laser is about 20% at most and LSPs involve very intense radiation resulting large energy loss.[16]

Figure 14 illustrates the schematic of the stabilization by using LSP. The LSP placed in a discharge tube has enough electron density to absorb the RF power. The absorption front would propagate toward all radial direction along the flow and form a axisymetrical ICP.

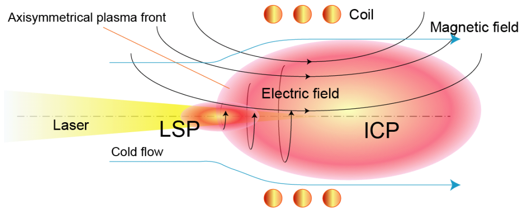

Figure 14. Schematic of the stabilization of ICPs by using LSPs.

B. Experimental setup and ICP torch modification

In order to introduce the laser irradiation into the discharge tube, a laser induction window and a laser exit window were installed on the torch. A zinc selenide (ZnSe) disk with anti-reflection coating was used as the windows. The aperture diameter of the window was 35 mm and the thickness was 5 mm. The ZnSe window has high transmission efficiency over the far infrared region involving around 10.6 mm wavelength. Figure 15 shows a schematic of the experimental apparatus. The condenser lens was mounted on a one-axis stage, which is movable in the laser beam direction. A rod made of stainless steel was used as the source of the initial electron emission. After the ignition the LSP was moved into the discharge tube with a movement of the focal point.

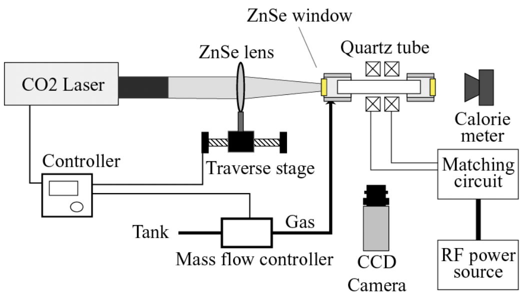

Figure 15. Schematic of the experimental setup.

C. Experimental results

Figure 16 shows images of the ICP stabilized by a LSP with laser power of 700 W and RF power of 700 W. The CW laser device has fluctuations in its laser output so that the LSPs are oscillated along the laser beam axis.[17] Since the ICP was also oscillated with the LSP oscillation, the generated ICP can be said to be stabilized by the LSP. As the mass flow rate was decreased with a fixed pressure, the ICP became instable and disappeared because of the limitation of the LSP generation. Therefore it was successfully demonstrated that the LSP had a stabilizing effect of ICP.

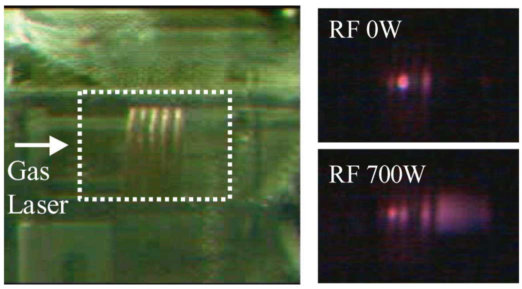

Figure 16. Images of the LSP (upper) and stabilized ICP (lower).

D. Double tube configuration

The fractional laser absorption power was about 45 % of the incident laser power. The laser absorption by the LSP depends on the flow parameters such as the flow velocity and the pressure of the flowfield. Hence there is the possibility that the pressure and the scale of the ICPG affect the LSP operational conditions.

The LSPs are generated at an equilibrium position where the propagation velocity of the LSP equals to the velocity of the flowing flow. The propagation velocity is thought to be proportional to the laser intensity so that the larger flow velocity brings the LSP close to the focal point of the condensing laser light. In the previous study, it was found that the energy conversion efficiency could be increased by the increase in the flow velocity.[16] Therefore it would be significant that the flow parameters of the LSP and the ICP are independently controlled.

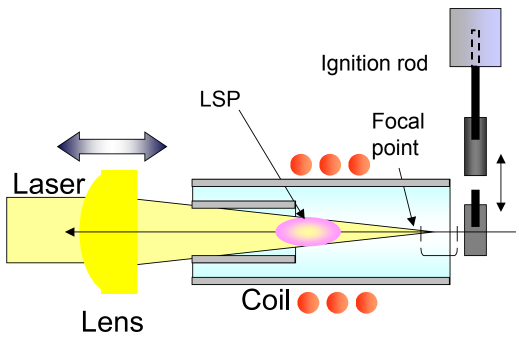

Figure 17. Schematic of the double tube configuration.

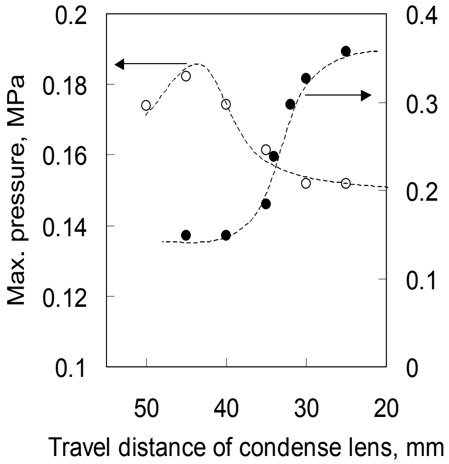

Figure 18. Schematic of the double tube configuration.

In this study, a double tube configuration was tried, which was expected to produce partially fast flow field in the center axis of the discharge tube (Fig. 17). The LSP is sustained in the fast flow field of which flow velocity dose not depend on the scale of the ICPG so that the stabilization effect is expected to be applied to a wide range of the flow field parameters. The inner diameter of the inner tube was 17 mm.

So far, as far as the authors know, there has been no research that describes the laser plasma generation in the double tube configuration. First of all, the operational behavior of the LSP was investigated as a function of the travel distance of the condensing lens. The LSP was brought closed to the inner tube with the movement of the condensing lens and was sustained in the inner tube at the travel distance of 40 mm. Figure 18 shows the maximum operational pressure with the mass flow rate of 15 slm and the laser power of 700 W. It was found that the LSP approach to the inner tube increased the maximum operational limit of the pressure gradually and the limit reached to the maximum value at the travel distance of about 40 mm. Then the minimum operational limit of the mass flow rate was measured with the pressure being fixed at 0.14 MPa. Experimental shows that the more closed to the inner tube, the lower the operational limit in the mass flow rate was. These results confirmed that the operational limit can be released not only by putting LSPs into the inner tube, but also by LSPs being sustained near the inner tube.

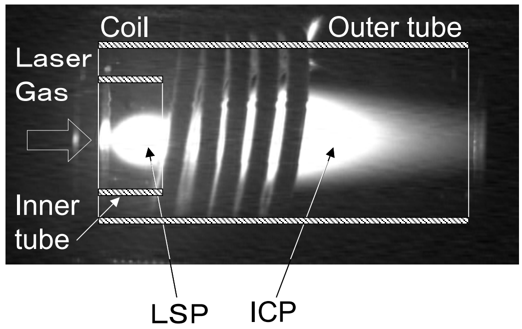

Figure 19. Schematic of the double tube configuration.

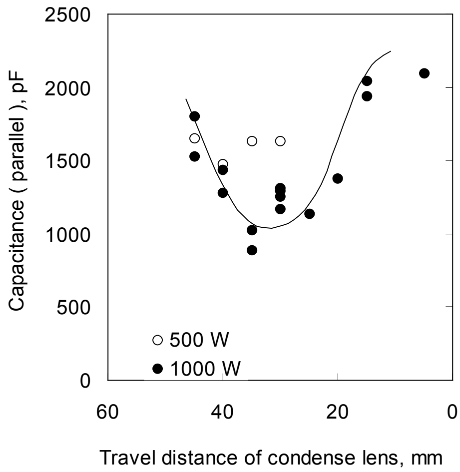

Figure 20. Schematic of the double tube configuration.

Figure 19 shows an image of the stabilized ICP by the LSP in the inner tube. The RF power and the laser absorbed power was 920 W and 280 W respectively. The image observes that the tail of the LSP was heated by the RF field, and high temperature region propagated toward radial direction along the flow.

The coupling of the load coil and the ICP increase the effective resistance of the load coil resulting the decrease in the capacitance of the C_p for impedance matching. They can be expressed as follows;

$$R' = R + \frac{M^2 \omega^2 R_p}{R_p^{\ 2} + \omega^2 L_p^2} \tag{4}$$

$$C_p = \frac{1}{50\omega}\sqrt{\frac{50}{R'} - 1} \tag{5}$$

Here M is the Mutual inductance between the load coil and equivalent coil of an ICP. It is expressed that the stronger coupling, i.e. the larger M, increase equivalent resistance and enable efficient energy transmission to the plasma. Then one can infer the condition of the coupling from the capacitance. Figure 20 shows the capacitance for impedance matching as a function of the travel distance. It was found that the strongest coupling was obtained when the LSP was located in the load coil.

V. Discussion

In this study, fundamental studies on an atmospheric inductively coupled plasma generator for high-enthalpy and high-stagnation pressure flow were conducted. Fist of all, the operational characteristics of atmospheric inductively coupled plasma was investigated in detail. We successfully demonstrated the generation of ICPs with the pressure of more than 1 atm. It was found that the operational conditions strongly depend on the design of the tangential flow injection ring and the pressure.

It was also successfully demonstrated that Laser Sustained Plasma (LSP) could be applied to the ICP stabilization. Placing the LSP in the load coil enabled to generate an ICP without the tangential flow injection. Since the stabilized ICP was influenced by the operational conditions of the LSP, it can be expected that the ICP can be produced if only the flow field parameters are within the operational condition of the LSPs. Especially using the double tube configuration will provide a wide range of the capability to stabilize the ICPs.

Though it was demonstrated that the ICP could be produced in a relatively high-pressure atmosphere, the plasma involved strong radiation resulting large energy loss and rapid decay of the flow enthalpy due to the intense radiation that is inferred from the images. Though the next study has to be devoted to evaluation of the flow enthalpy after a Laval nozzle, there would be a breakthrough to produce high-enthalpy and high-pressure flow efficiently.

So far Herdrich et.al. investigated the plasma acceleration by using a nozzle and obtained the high plasma enthalpy with high velocity of the jet.[18] However their interests was focused on the Mars entry simulations, where the stagnation pressures which are a typical value for the Mars relating missions are in the order of 1 kPa. As to the acceleration of an atmospheric ICP, Sember et.al. investigated that the property of a supersonic argon and argon–hydrogen (3–5%) plasma jet generated by an induction plasma torch by means of the methods of optical emission spectroscopy.[19] They described the nonequilibrium characteristics of the supersonic flow precisely, while the thermodynamic characteristics such as flow enthalpy and the total pressure were not measured. It is thought that the acceleration of the atmospheric ICPs would be the next issue.

Acknowledgement

This work has been supported partly by Research Fellowships of the Japan Society for the Promotion of Science for Young Scientists. The author would like to thank the JSPS for the support.

References

[1]Solar System Exploration Survey Space Studies Board, "New Frontiers in the Solar System: An Integrated Exploration Strategy," THE NATIONAL ACADEMIES PRESS, Washington DC, 2003.

[2]Seiff, A., et. al., "Measurements of Thermal Structure and Thermal Contrasts in the Atmosphere of Venus and Related Dynamical Observations: Results From the Four Pioneer Venus Probes" *J. Geophysical Research*, Vol. 85, No. A13, 1980, pp. 7909-7933.

[3]Laub, B., and Venkatapathy, E., "Thermal Protection System Technology and Facility Needs for Demanding Future Planetary Missions," Proceedings of the International Workshop on Planetary Probe Atmospheric Entry and Descent Trajectory Analysis and Science, I - 6.1 , Lisbon, Portugal, 2003.

[4]Zoby, E.V. "Empirical stagnation-point heat-transfer relation in several gas mixtures at high enthalpy levels," NASA-TN D-4799, 1968.

[5]Herdrich, G., Auweter-Kurtz, M., and Kurtz, H., "New Inductively Heated Plasma Source for Reentry Simulations" *Journal of Thermophysics and Heat Transfer*, Vol. 14, No. 2, 2000, pp. 244-249.

[6]Yamada, T., and Inatani, Y., "Inductively-coupled High Enthalpy Flow Generator for Planetary Entry Probes," Proceedings of the 24th International Symposium on Space Technology and Science, 2004-e-21 , Miyazaki, Japan, 2004.

[7]Bottin, B., Carbonaro, M., Zemsch, S., and Degrez, G., "Aerothermodynamic design of an inductively doupled plasma wind tunnel" *AIAA 97-2498*, 1997.

[8]Thope ,M.L., et.al. "Induction Plasma Heating," NASA-CR 1343, 1969.

[9]Vegel, C.E., Pole, J.W., and Dundas, P.H., "Radiation Measurements and Low Frequency and High pressure Investigations of Induction Heated Plasma," NASA-CR 1807, 1971.

[10]Poole, J.W., Vogel, C.E., " Induction Torches and Low Frequency Tests," NASA-CR 2053, 1972.

[11]Herdrich, G., Auweter-Kurtz, M., and Kurtz, H., Laux, T., Schreiber, E., "Investigation of the Inductively Heated Plasmagenerator IPG3 Using Injection Rings of Different Geometries" *AIAA*-2000-2445.

[12]Ito, T., et.al., "Heating Tests of TPS samples in 110 kW ICP-heated wind tunnel," Proceedings of the 24th International Symposium on Space Technology and Science, 2004-e-20 , Miyazaki, Japan, 2004.

[13]Yabuta, H., Miyahara, H., Watanabe, M., Hotta, E., and Okino, A., "Design and evaluation of dual inlet ICP torch for low gas consumption," *Journal of Analytical Atomic Spectrometry*, Vol.17, 2002, pp.1090–1095.

[14]Gutsol, A., Larjo, J., and Hernberg, R., "Comparative Calorimetric Study of ICP Generator with Forward-Vortex and Reverse-Vortex Stabilization," *Plasma Chemistry and Plasma Processing,* Vol. 22, No. 3, 2002, pp.351-369.

[15]Kemp, N.H., and Lewis, P.F., "Laser-heated thruster –Interim report," NASA-CR 16165, 1980.

[16]Uehara, S., Inoue, T., Komurasaki, K., and Arakawa, Y., "An Experimental Study on Energy Conversion Process of an in-Space CW Laser Thruster;" Proceedings of the 3rd International Symposium of Beamed Energy Propulsion, Troy, NY, USA, 2004 (to be published).

[17]Inoue, T., Ijiri, T., Hosoda, S., Kojima, K., Uehara, S., Komurasaki, K., and Arakawa, Y., "Oscillation phenomenon of laser-sustained plasma in a CW laser propulsion," *Vacuum*, 73, 2004, pp.433-438.

[18]Hdrich, G., Auweter-Kurtz, M., Endlich, P., and Kurtz, H., Y., "Mars Entry Simulation Using an Inductively Heated Plasma Generator," *Journal of Propulsion and Power*, Vol.40, No.5, 2003, pp.690-693.

[19]Sember, V., Gravelle, D.V., and Boulos, M.I., "Spectroscopic study of a supersonic plasma jet generated by an ICP torch with a convergent–divergent nozzle," *Jounal of Physics D: Applied Physics*, Vol.35, 2002, pp.1350-1361.